LIP-STUDENTS-22-11

Development of Hybrid ^{10}B – RPC based neutron detectors

Carolina Fernandes[1,a]

[1] *Universidade de Coimbra, Coimbra, Portugal*

Project supervisor: Luís Margato and Andrey Morozov

October 19, 2022

Abstract. Neutrons are uncharged particles with magnetic moment, and this gives them some important characteristics, such as, e.g., they can deeply penetrate the matter and sense magnetic phenomena in materials, that makes them useful in many scientific methods, for example in imaging and neutron tomography techniques. However, the same aspect that enables such powerful applications makes their detection difficult. Here we describe a type of detector for thermal and cold neutrons that combines Resistive Plate Chambers and $^{10}B_4C$ converters. We will use Monte Carlo simulations performed with ANTS2 and Geant4 toolkits to investigate how the $^{10}B_4C$ layer thickness and the angle of incidence of neutrons on it affect the detection efficiency of a single RPC, our basic neutron detection unit. The design and assembly procedure of the ^{10}B-RPCs for a detector prototype is also described.

KEYWORDS: Neutron, RPC, Monte Carlo and Detector

1 Introduction

1.1 Thermal Neutrons

Thermal neutrons have an average energy of about 0.025 eV, corresponding to a De Broglie wavelength of 1.8 Å. This value is comparable to the distance between the atoms in solid matter thus, they are used to study the structure of condensed matter. Because of their high sensitivity to light elements and isotopes, e. g., deuterium, they are an important complement to the X-ray based techniques. Due to their magnetic moment, they are also a useful probe for studying magnetism.

Neutrons are not straightforward ionizing and they have generally to be detected through a nuclear reaction [1]. For a slow neutron to be detected first, a nuclear capture reaction must happen. Typically, such reaction results in the emission of charged particles which, in turn, can be detected due to their ionization effect. This is possible only with a few isotopes, such as, e.g., ^{10}B, ^{3}He, ^{6}Li, ^{155}Gd and ^{157}Gd. To choose the best option that will be used in a detector, the parameters to consider are the capture cross-section, that has to be high, and the type of reaction between the neutrons and the isotope, which should produce charged particles with high kinetic energy. This will allow a better discrimination of the background, including the gamma rays. Helium-3 has been the most used isotope because it has good results in these two parameters. However, the access to the ^{3}He is difficult now so it becomes quite impossible to use it in neutron detectors. One alternative that appears to be one of the best options is the ^{10}B. It has a relatively high cross-section and its natural abundance is high enough [2].

The reaction that happens between the neutrons and ^{10}B has a lithium and an alpha particle as products. The energy of the thermal neutron is low so incoming linear momentum is very small, consequently the reaction products also have net momentum near to zero. This makes the products to be emitted in opposite directions according to the expressions below expressing the neutron capture reaction $^{10}\mathrm{B}(n,\alpha)^{7}$ [1],

$$^{10}\mathrm{B} + \mathrm{n} \rightarrow {}^{7}\mathrm{Li}\,(0.84\,\mathrm{MeV}) + {}^{4}\mathrm{He}\,(1.47\,\mathrm{MeV}) + \gamma\,(0.48\,\mathrm{MeV}) \quad (94\%)$$
$$^{10}\mathrm{B} + \mathrm{n} \rightarrow {}^{7}\mathrm{Li}\,(1.02\,\mathrm{MeV}) + {}^{4}\mathrm{He}\,(1.78\,\mathrm{MeV}) \quad (6\%)$$

This reaction is crucial for the operation of the detector that will be described in the current paper. Boron-10 appears in the solid state as one of the components of $^{10}B_4C$ (boron carbide) [3].

1.2 Hybrid ^{10}B – RPC

Resistive Plate Chambers (RPC) are gaseous parallel-plate detectors that combine good spatial and time resolution. The standard RPC are used since 1981. An RPC consists of two resistive parallel plates, separated by a gas gap of a few millimeters. A high uniform electric field strength is defined in the gas gap by applying a high voltage in the outer surfaces of the resistive plates. The plates are typically coated with conductive ink to guarantee a uniform potential along the entire surfaces. The operation principle is based on the ionization processes occurring in the gas gap. The strong uniform electric field between the resistive plates causes electrons to separate from ions, and accelerates them generating more electrons via ionization, in the so-called electron avalanches. The drift of both, electrons, and ions will induce signals on pick-up electrodes on top of the external sides of the resistive plates [4].

In the detector described in this paper the RPCs have a double gap configuration [5] and are composed by two resistive plates, made from float glass (the anodes at ground potential) and, between them, one metallic conductive plate, made from aluminum (the cathode keep at a negative potential). The gas gap's, with a width of ~0.35 mm, are usually filled with tetrafluoroethene CH_2FC_3 at atmospheric pressure. The cathode is coated by a thin (~1 - 2 μm) layer of $^{10}B_4C$. Without this layer the detector is

[a] e-mail: c03fernandes@gmail.com

almost transparent to the neutrons . The alpha or ^{7}Li particles from the neutron capture reaction in the layers of $^{10}B_4C$, can escape to the gas gap and generate ionization. This will start electron avalanches leading to the induction of signals on pick-up electrodes. The electronic readout and processing of the signals will finally allow the neutron detection process to be accomplished. The position sensitivity in this type of detector can be enabled by installing two arrays of orthogonal signal pick-up strips facing each anode-plate. This is the so-called hybrid double gap ^{10}B-RPC [5].

The double gas gap RPC is one of the most favorable designs because it allows to use $^{10}B_4C$ double coated aluminum cathodes.

Typically, one single gap ^{10}B-RPC shows only about 5% neutron detection efficiency to normal-incidence neutrons. This value can be increased to values above 50% by opting for a multilayer detector design with double gap RPCs stacked. In this configuration the arrays of signal pick-up strips can be shared by two gas gaps and the cathode signals used to identity the triggered RPC.

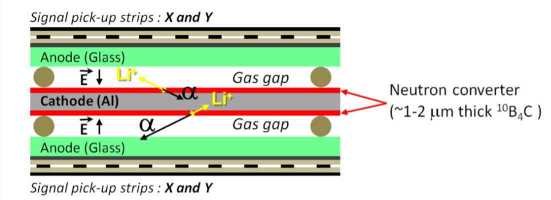

Figure 1. Double-gap RPC configuration: a single metallic cathode, lined on both sides with $^{10}B_4C$ neutron converter, is shared by two anodes [5].

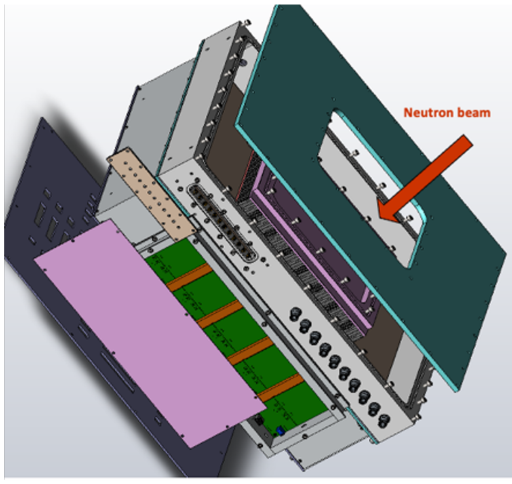

Figure 2. Exploded view of the detector prototype.

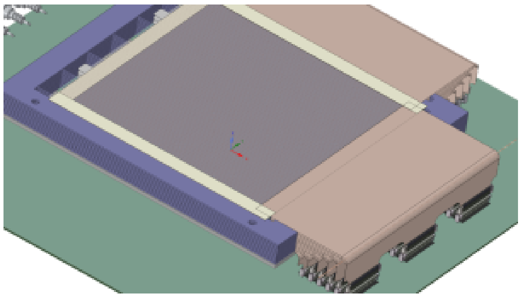

Figure 3. Top view inside the prototype showing the stack of ten ^{10}B-RPCs and the 2D-Flex PCBs with pick-up strips for the position readout.

2 ^{10}B-RPCs for a multilayer detector prototype

A detector prototype aiming to demonstrate the capability of the ^{10}B-RPC neutron detection technology for detectors with four dimensional (4D) capability (X, Y, Z and time) is being build. The concept can be applied, e.g., in the design of high precision neutron detectors requiring the measurement of both, the position and TOF (time-of-flight) of neutrons, and in time- and energy-resolved neutron imaging.

To offer a high detection efficiency (> 50%) to thermal and cold neutrons it was chosen a multilayer design with ten double gap ^{10}B-RPCs. Figure 2 shows an exploded view of the prototype. For an inside view see Figure 3, showing the stack of the ten RPCs.

In this section I will describe in detail the structure of the double gap ^{10}B-RPCs builds for the prototype. The assembly procedures of the ^{10}B-RPCs, in whose construction I participated, will be also described.

2.1 Structure of the ^{10}B-RPCs

The ^{10}B-RPCs have a double gap configuration (see Figure 1 in section 1.2). The cathode plates with an area of 190 mm x 190 mm are made from 0.3 mm thick aluminum (Al 5756). The Al-plates were coated on both sides with a thin layer of $^{10}B_4C$ with a ^{10}B enrichment level of ~97%. These coatings were performed in the neutron detectors group at the European Spallation Source (ESS) in three different thicknesses: Th1 $\approx$ 0.4 μm, Th2 $\approx$ 0.6 μm and Th3 $\approx$ 2.2 μm. The Aluminum plates with a $^{10}B_4C$ thickness Th1 are assembled on RPC1 to RPC3, with Th2 on RPC4 to RPC7 and with Th3 on RPC8 to RPC10. The anode plates with an area of 200 mm x 200 mm are made from 0.33 mm thick soda lime glass. One of the faces of the glass plates (external surface) is lined with a 0.05 mm thick layer of resistive ink. This ink layer is intended to apply a uniform potential over the entire external surface of the glass-plates. To guarantee a uniform gas gap width between the two anode glass-plates and the cathode Al-plate, a 0.28 mm diameter PEEK monofilament is used as spacer. The PEEK spacers, Al-plate and 2 glass-plates, forming a double gap RPC, are hold by a frame made from 1.65 mm thick FR4 (see Figure 4).

2.2 Assembly procedures

The RPCs are assembled in a clean room to guarantee a very clean environment. And this to avoid the presence of particles of dust in the gas gaps, which can result to an increase of the dark counting rate and, in the limit, in a malfunction of the RPCs. The internal face (surface facing the gas gap) of the glass-plates is cleaned first with a glass cleaner solution with ammonia and then with methanol. To remove any stuck particles, the glasses are further blown with filtered compressed air. This last procedure is also used on the Al-plates and FR4-frames.

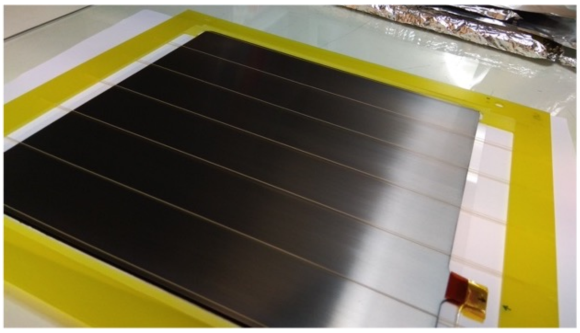

Figure 4. Double gap ^{10}B-RPC: frame made from FR4 holding the PEEK spacers and an Al-plate coated on both sides with $^{10}B_4C$.

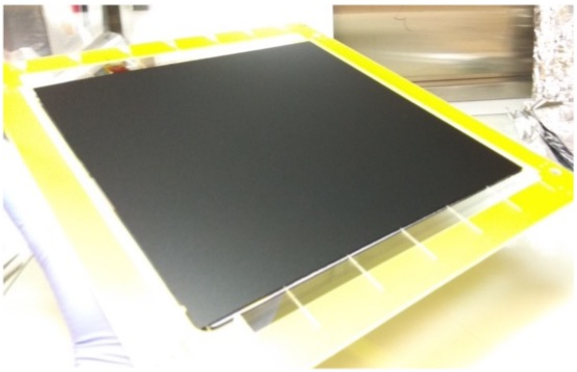

Figure 5. Double gap ^{10}B-RPC: glass plates already on top of the spacers with the Al-plate in between.

We start by aligning the PEEK-spacer segments on the FR4-frames. The ends of these segments are fixed to the frames in the holes dedicated for this purpose with hot glue. To avoid the FR4-frame warping, we must ensure that all spacer segments exert the same tension on it. To ensure this, all spacers were stretched with the same weight. The next step is the insertion of the Al-plates between the spacers (see Figure 5). To prevent damage on the ^{10}B$_4$C layers during this procedure, the surfaces of the aluminum plates are protected with lint-free clean room wipes. Finally, both glass-plates are aligned on each side of the FR4-frame, on top of the spacers defining a uniform gas gap width of 0.28 mm (see Figure 5). There is a recess in the FR4-frames that prevents the plates from sliding. For the glass-plates do not fall out, we just apply a strip of 0.05 mm thick Kapton tape to their edges. This is a non-destructive construction, which allows us to disassemble and reassemble the double gap RPCs whenever needed, e.g., for inspection and replacement of the glass, aluminum plates or spacers.

The same assembly methodology was repeated for all the ten RPCs that constitute the detector.

3 Simulation study

Detection efficiency is an important parameter of the detector, and it has to be as high as possible. To increase this parameter in this type of the detector there are two options: one can optimize the thickness of the converter layer or the angle between the neutron beam and the RPC. To test these two options, I perform a Monte Carlo (MC) simulation in Geant4 using ANTS2 interface. In this paper the results are obtained with simulation performed using the QGSP_BERT_HP physics list (HP means high precision neutron model). The neutron is considered detected when the products of the neutron capture reaction are depositing at least 100 keV in the gas gap. I set an energy of 0.025 eV for the neutrons in the beam which corresponds to a neutron wavelength of 1.8 Å.

3.1 Efficiency versus converter thickness

With the propose to find the optimal thickness of the converter I implement a detector design with just one hybrid double-gap ^{10}B-RPC. If the ^{10}B$_4$C converter layer is too thick the probability of the capture reaction is high, but the products can barely reach the gas gap. In other hand if the converter is too much thin the probability of the reaction becomes very low. So, the optimal thickness represents the best compromise between these two conditions.

3.2 Efficiency versus RPC tilt angle

To test the influence of the tilt angle of the RPC in an inclined geometry, on the neutron detection efficiency, I choose a detector design with one single-gap ^{10}B-RPC (RPC with the cathode coated with $^{10}B_4C$, in only one of the faces). In this geometry the distance that the neutrons travel inside the converter increases according to 1/sin(θ) [6], (θ represents the angle between the direction of incident neutrons on the RPC and the plain of the ^{10}B$_4$C layer).

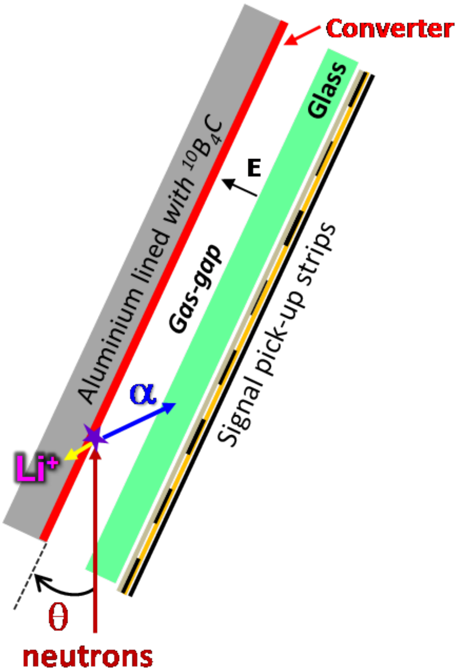

Figure 6. Design of a single-gap ^{10}B-RPC at an inclined geometry[5].

3.3 Multilayer RPC

As already was mentioned above, a detector prototype is being assembled with a ^{10}B-RPC stack, so it is essential to know if the optimal thicknesses of all the converters will be equal and if there is advantage of opting for different thicknesses. To better understand this a simulation was performed with a detector design having a stack of 3 RPCs. The main goal was to reach the maximum efficiency of the stack, but at the same time with the individual efficiencies of each RPC to be as equal as possible to each other. This flatness of the efficiencies allows to improve the counting rate capability of the detector. This is because, it let a more equal distribution of the totality of detected events by all the RPCs, avoiding premature saturation of the ones facing the neutron beam. With the help of an optimization method I compute the best compromise between total efficiency and flatness. The first step was to find two equations, one for the total efficiency and other for the flatness, in both equations the variables are the three converter thicknesses. After that, to use the minimizers method we had to find a function in which the variables are total efficiency and flatness. With this function we used computationally the minimizers method to find three thicknesses that give us the minimum value of the function. This method tries all the directions that can take in a three-dimensional space, with the three-axis representing the three thicknesses, to find the set of thicknesses that gives the minimum of the cost function [6].This minimum will be the optimal result. It is helpful and quickly when the variables are related.

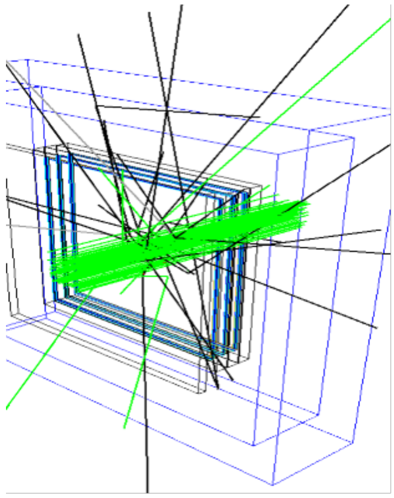

Figure 7. Design of the detector implemented in ANTS2 and G4 used in the optimization process.

Equations, used in minimizers method:

Efficiency of each RPC: e_1, e_2, e_3

$$\text{Total efficiency: } E_T = e_1 + e_2 + e_3$$

$$\text{Flatness } F = (e_1 - e_2)^2 + (e_1 - e_3)^2 + (e_2 - e_3)^2$$

$$\text{Cost function: cost} = 100F - E_T$$

4 Results and discussion

The graph bellow (Figure 8) shows that the detection efficiency increases with the converter thickness, until it reaches a peak. The peak represents the range of the optimal values of the thickness. After the peak the detection efficiency reduces and approaches asymptotically a non-zero plateau value.

The reason for the plateau is that the reaction products can reach the gas gap only from a certain thickness. After a certain depth value the reaction products are stopped by the $^{10}B_4C$ layer itself and the captures start to become invisible.

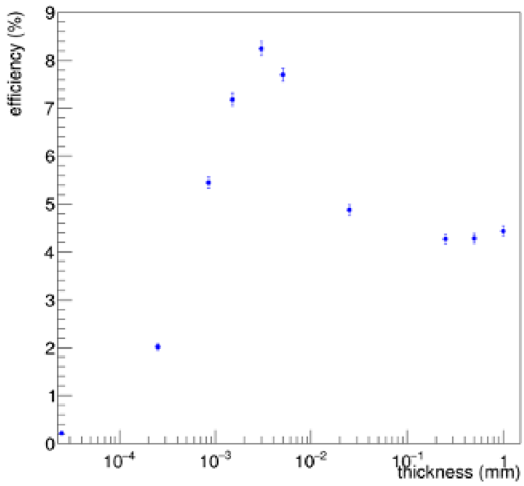

Figure 8. Graph of the efficiency versus the thickness of the $^{10}B_4C$ converter.

In the Figure 9 it is evident that the efficiency increases exponentially with the tilt angle of the RPC relative to the direction of neutron incidence. This was an expected result having in mind the dependence of the detection efficiency with the expression $1/\sin(\theta)$ on the tilt angle of the RPC.

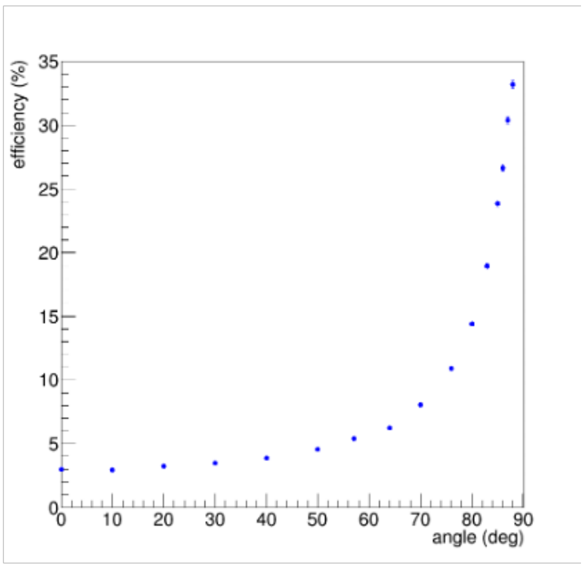

Figure 9. Dependence of the efficiency on the angle (θ) between the direction of incident neutrons and the plain of the RPC. In abscissa axis is represented the complementary angle of θ.

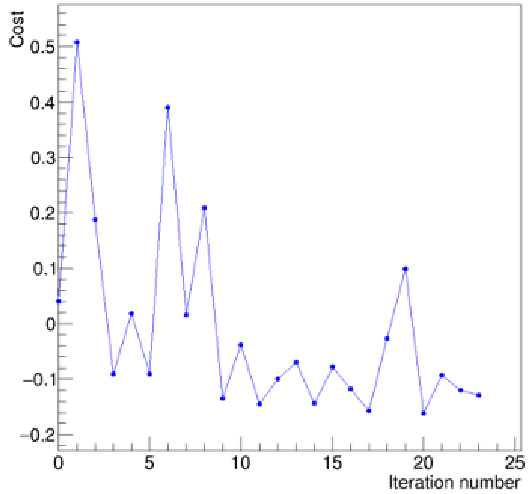

Figure 10. Cost function value returned to the optimizer after a certain number of iterations.

Figure 10 represents the iterations that the minimizer method had to do, to find the values of the three thicknesses of the converter layers for the three RPCs. The iteration that represents the optimal value is the iteration number twenty. The results for the thicknesses of the $^{10}B_4C$ layers are:

First RPC: 0.92 μm;
Second RPC: 1.06 μm;
Third RPC: 1.35 μm;

5 Conclusion

The configuration of the ^{10}B-RPCs is presented and their basic working principle for the detection of thermal neutrons is described. It is also presented the structure of the ^{10}B-RPCs for a prototype that is being built and its assembly procedure explained.

Study of how a detector performs even before it is assembled is crucial to assists in its design, to know how we should build it to reach the maximum performance possible. With this objective, it is performed an MC simulation to compute the optimal thicknesses of the $^{10}B_4C$ neutron converter layers that can improves the neutron detection efficiency.

For one double gap ^{10}B -RPC, with neutrons at normal incidence with respect to the converter surface, it is determined that the converter thicknesses maximizing the detection efficiency (λ = 1.8 Å) is in the range 2 – 4 μm, resulting in an efficiency of ~ 8.5%. The simulation results also show that tilting the RPC of a certain angle with respect to the direction of neutron incidence is an effective way to increase the efficiency, although it is mechanically more demanding to assemble a detector in this type of geometry.

It is also exemplified by simulation of a stack of three ^{10}B-RPCs that, an optimal thicknesses for each individual converter layer in the ^{10}B-RPCs of a multilayer detector can be defined. This allows achieving the best compromise between maximum detection efficiency and flatness. Such an optimization is a crucial step to define the best detector design to achieve, e.g., the highest possible detection efficiency and count rate capability.

Acknowledgements

A special thanks to the internship supervisors, Luís Margato and Andrey Morozov, for the chance that they given to me to learn at a theoretical and a practical level about neutron detection and about simulation processes. Thanks to LIP for this enriching and unique opportunity.

References

[1] G. F.Knoll, Book (2010)
[2] K. Zeitelhack, Neutron News 23 (2012)
[3] C.H. et al, J. Appl. Phys. (2012)
[4] G. Cattani, Conference Series, Volume 280 (2011)
[5] L. Margato, A. Morozov, JINST 13 P08007 (2018)
[6] A.M. et al, JINST 15 P03019 (2020)